Energy, Mines and Resources Canada
Earth Physics Branch

Énergie, Mines et Ressources Canada
Direction de la physique du globe

This document was produced by scanning the original publication.

Ce document est le produit d'une numérisation par balayage de la publication originale.

Geomagnetic Service of Canada

A THREE-COMPONENT AEROMAGNETIC SURVEY OF EASTERN CANADA

G.V. Haines and W. Hannaford

Geomagnetic Series
Number 16
Ottawa, Canada 1980

Energy, Mines and Resources Canada
Earth Physics Branch
1 Observatory Crescent
Ottawa Canada
K1A 0Y3

Énergie, Mines et Ressources Canada
Direction de la physique du globe
1 Place de l'Observatoire
Ottawa Canada
K1A 0Y3

Geomagnetic Service of Canada

A THREE-COMPONENT AEROMAGNETIC SURVEY OF EASTERN CANADA

G.V. Haines and W. Hannaford

Geomagnetic Series
Number 16
Ottawa, Canada 1980

© Minister of Supply and Services Canada 1980

Available in Canada through

Authorized Bookstore Agents
and other bookstores

or by mail from

Canadian Government Publishing Centre
Supply and Services Canada
Hull, Quebec, Canada K1A 0S9

Earth Physics Branch,
Energy, Mines and Resources Canada,
1 Observatory Crescent,
Ottawa, Canada K1A 0Y3

Catalogue No. M74-32/16
ISBN 0-660-50719-6
ISSN 0704-3015

Canada: $2.00
Other Countries: $2.40

Price subject to change without notice.

© Ministre des Approvisionnements et Services Canada 1980

En vente au Canada par l'entremise de nos

agents libraires agréés
et autres librairies

ou par la poste au:

Centre d'édition du gouvernement du Canada
Approvisionnements et Services Canada
Hull, Québec, Canada K1A 0S9

Direction de la physique du globe,
Énergie, Mines et Ressources Canada,
1 Place de l'Observatoire,
Ottawa, Canada K1A 0Y3

N° de catalogue M74-32/16
ISBN 0-660-50719-6
ISSN 0704-3015

Canada: $2.00
Hors Canada: $2.40

Prix sujet à changement sans avis préalable.

CONTENTS

Abstract..... v

Introduction..... 1

Navigation..... 1

Horizontal fields, angles, and coordinate system..... 3

Calibration and aircraft-field corrections, permanent and induced..... 4

1. General Case..... 4

2. No Z variation over swings..... 4

3. No H or Z variation over swings..... 5

Calibration and aircraft-field corrections, permanent only..... 6

Swing-derived corrections..... 6

Consistency-derived corrections for Z..... 8

Consistency of data from the two magnetometer systems..... 9

Presentation of data..... 9

Acknowledgments..... 11

References..... 11

ABSTRACT

A three-component airborne magnetic survey of central and eastern Quebec, Davis Strait, the Atlantic Provinces, and adjacent areas of the Atlantic Ocean was carried out in late 1976. The average flight line spacing was 74 km and the average altitude was 4.6 km above sea level. Only data considered to be relatively free of disturbance fields are presented. The data were averaged over 30 seconds of time, or approximately 3.5 km of flight track. The International Geomagnetic Reference Field (IGRF) was removed from these averages, and the resulting residuals plotted as profiles. A 3rd degree polynomial was fitted to the survey data by least-squares. Contour plots of the polynomial field minus the IGRF are given.

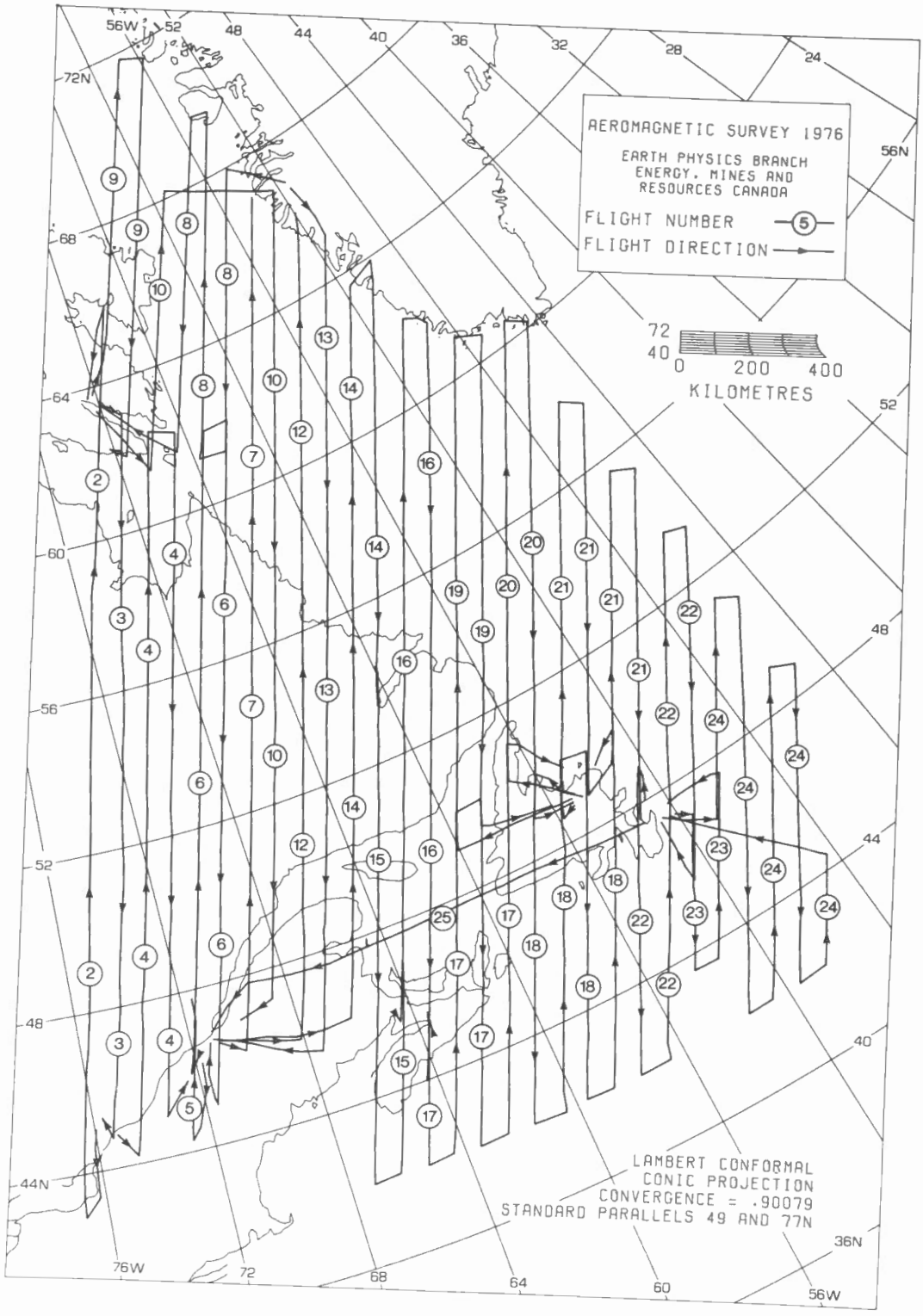

Fig. 1 Flight lines of the Earth Physics Branch 1976 3-component aeromagnetic survey of eastern Canada. Flight numbers are circled and arrowheads indicate the direction of flight. The survey was carried out between August 31 and October 15, 1976, at an average altitude of 4.6 km.

A THREE-COMPONENT AEROMAGNETIC SURVEY OF EASTERN CANADA

G.V. Haines and W. Hannaford

INTRODUCTION

In 1976, between August 31 and October 15, the Earth Physics Branch carried out an airborne three-component magnetic survey over central and eastern Quebec, Davis Strait, New Brunswick, Nova Scotia, Prince Edward Island, Newfoundland, and adjacent areas of the Atlantic Ocean. An index map of the survey flight lines is shown in Figure 1.

The aircraft used was a DC-6, chartered from Conair Aviation. Approximately 85,000 kilometres were flown, of which about 23,000 were test, ferry, and calibration flights.

The 62,000 line-kilometres over the main survey area were flown at an average fight-line spacing of 74 km, and at altitudes ranging from 3.0 to 4.9 km (the average being 4.6 km). The area covered was 4.5×10^6 km^2.

The magnetometer system consisted of two independent magnetometers: a proton precession sensor was mounted in a stinger at the rear of the aircraft and a gyro-stablized, three-axis fluxgate sensor was mounted at the rear of the aircraft cabin. The former gave the total field F, and the latter gave the declination D, horizontal intensity H, and vertical component Z.

For detailed descriptions of the platform, magnetometers, data-acquisition system and the on-board minicomputer system, see Haines and Hannaford (1974 and 1978).

NAVIGATION

The aircraft was equipped with two Litton LTN-51 inertial navigation systems (INS). One of these proved to be consistently more accurate than the other, and the better system was used as the principal instrument of navigation while the other served a back-up role. Both systems operated continuously through each flight except for flight 23 when the primary INS became inoperative shortly after takeoff.

The INS control panel has a keypad and two digital displays for the input and output of navigational information. Before takeoff the navigator inputs the values of latitude and longitude for the aircraft's position at that time, for its final destination, and for up to nine waypoints along the desired path. Every second thereafter, the INS computes the new latitude and longitude, true track angle and ground speed, and true heading and drift angle to next waypoint. The type of information to be presented on the INS dual display is selectable in pairs. Latitude and longitude are given in degrees and minutes to the nearest tenth of a minute; speed is given in knots and distances in nautical miles. New values appear every second unless the HOLD button is depressed.

Latitude and longitude indicated by both systems were logged every ten minutes, as a rule, together with the other INS outputs.

When identifiable landmarks were visible, the aircraft's actual position was determined from time to time by map reading. If the INS position was found to be in error by more than two or three nautical miles, the true values of latitude and longitude were inserted via the keypad, and an "update" command was given. The effect of this procedure is to eliminate the error which accumulates in the INS positions between one update and the next.

Immediately after each flight the aircraft was parked in an accurately known position and the corresponding INS position was logged. The distance in nautical miles between these two positions, defined as the terminal error, was then computed by the INS upon insertion of the true latitude and longitude. In addition the INS computes the distance between true final position and that which it would have indicated if no in-flight updates had been performed. The latter is defined as trip error; when

divided by the duration of the flight it yields the average error rate. The mean of the error rates computed for 24 flights was 1.5 km/hr, and the standard deviation was 1.1.

An indication of the accuracy of the INS positions was obtained by using the terminal errors together with those determined from visual in-flight checks. In both cases the error is influenced by the preceding update, if there was one. The mean and standard deviation of 90 INS position errors so obtained were 5.9 and 4.8 km, respectively.

However, certain adjustments to the INS positions were made before the final assignment of geographical locations to the survey data. A linear adjustment was made to the positions which preceded an update, to remove the discontinuity which would otherwise appear. Also, where no updates were made but visual checks indicated a consistent offset in the INS positions, an adjustment was made accordingly. The resulting list, giving positions every 10 minutes and at times when the aircraft changed heading, was used as the basis for determining the location of the geomagnetic profiles presented here. Intermediate positions were interpolated on the assumption that the aircraft followed a great circle path at constant ground speed between two consecutive positions on the list.

The accuracy of the navigational information in its final form was then estimated by comparing the 66 in-flight visual fixes with the corresponding calculated positions. The mean and standard deviation of the indicated errors were 3.9 and 2.5 km.

In addition to supplying the information on which the location of the survey data was based, the primary INS also enabled the autopilot to keep the aircraft on course automatically by providing a voltage analog of the cross-track error which could be switched into the autopilot steering control.

On previous surveys a doppler system provided an independent means of navigation and also supplied ground speed and drift information to the magnetometer systems minicomputer (see Haines and Hannaford, 1978). For the 1976 survey reported here, these functions were performed by the second INS.

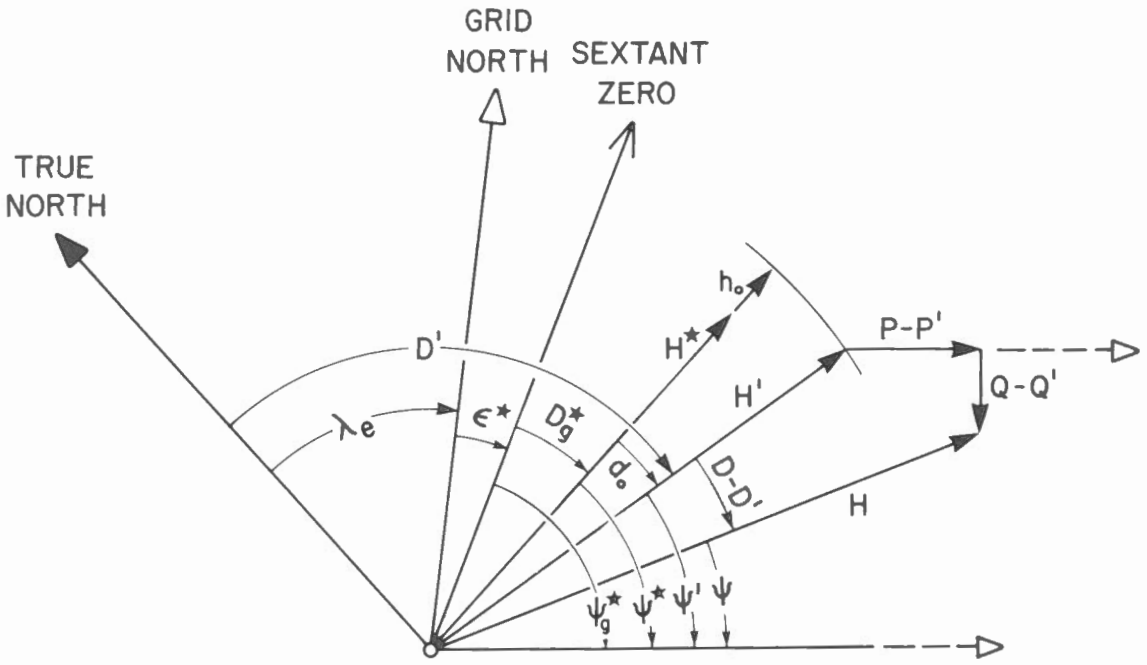

Fig. 2 Horizontal fields and reference directions relevant to the determination of D and H. The aircraft-field corrections P-P' and Q-Q' include the effects of both permanent and induced fields. However, the effects of induced fields cannot be distinguished from the effect of the angle d_o. The corrections are shown relative to H'; they can of course be expressed relative to H* as in Figure 3.

HORIZONTAL FIELDS, ANGLES, AND COORDINATE SYSTEM

Figure 2 shows horizontal fields and reference directions for the fluxgate magnetometer system. Primed quantities indicate elements of the "apparent" field (earth's and aircraft's fields combined). Starred quantities indicate measurements or values derived simply from measurements.

The east longitude λ_e is provided by the navigation system described in the last section. The angle ε^* is obtained from frequent monitorings of astronomical bodies during flight. Its determination has been explained by Haines and Hannaford (1978). It is a measurement of the angle between grid north (defined as the direction of true north plus east longitude) and the gyro direction. The angles ε and ε^* may differ by a few degrees, depending on the accuracy with which the sextant is aligned when initially mounted in the aircraft.

The angle D_g^* is a measurement of the angle D_g' between the gyro and apparent magnetic north (the direction of H'). The two angles may differ by a few tenths of a degree due to small errors in the digital voltmeter, precision voltage supply, and precision potentiometer.

The two correction differences $(\varepsilon - \varepsilon^*)$ and $(D_g' - D_g^*)$ are combined into the calibration correction angle d_o, which enables the apparent declination D' to be calculated:

$$D' = \lambda_e + \varepsilon^* + D_g^* + d_o \qquad 1$$

The measured horizontal field H* has to be corrected by the calibration constant h_o to give the apparent horizontal field H':

$$H' = H^* + h_o \qquad 2$$

Both D' and H' are corrected for aircraft fields to give the earth's declination D and horizontal field H.

The measurement of the angle ψ_g between the gyro and the roll axis of the platform is denoted by ψ_g^*. The angles differ, because of synchro error, by about a tenth of a degree. The platform and fluxgate sensor assembly is installed in the aircraft so that the roll axis of the platform is within a degree or two of the roll (or forward) axis of the aircraft. Hence ψ_g^* is within a couple of degrees of the aircraft's fore-and-aft axis and effectively denotes the heading of the aircraft relative to the gyro.

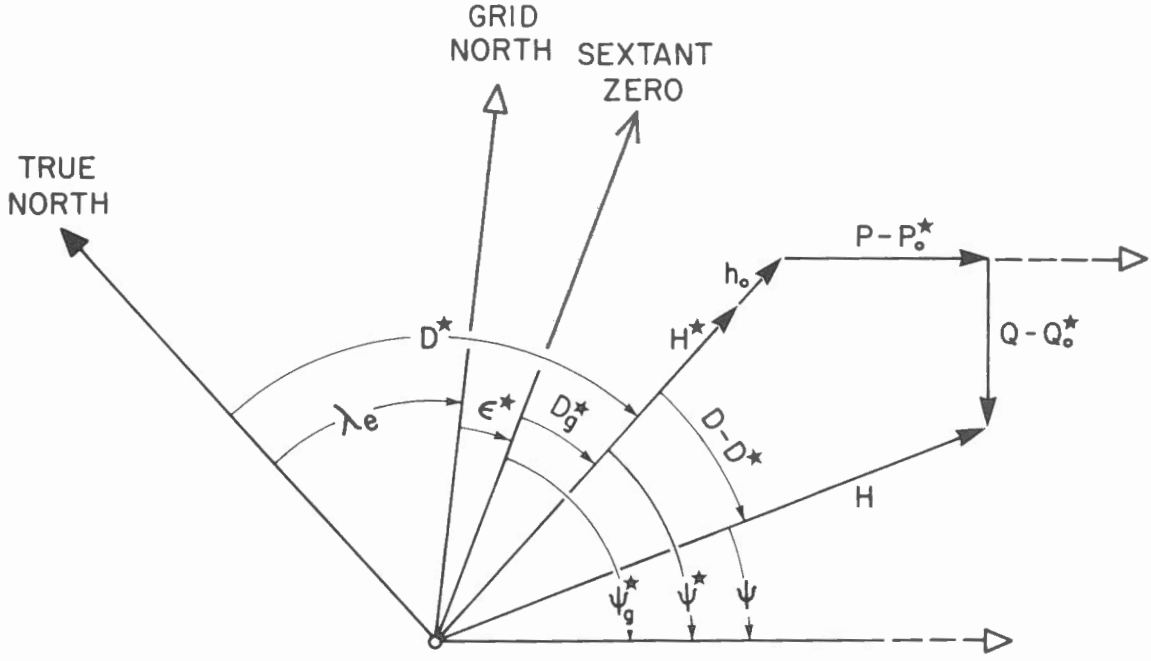

Fig. 3 Calibration and aircraft-field corrections relative to H*. The corrections $P-P_o^*$ and $Q-Q_o^*$ include the effect of the angle d_o (Figure 2) as well as the effect of permanent and induced fields.

For purpose of determining and removing aircraft fields, a coordinate system, fixed relative to the aircraft, is defined by means of the angle ψ_g^*. Adding ψ_g^* to the direction of the sextant zero defines the direction of the "P" coordinate; 90° clockwise from this is the "Q" coordinate. The P coordinate is thus within a few degrees of the aircraft's forward axis. In fact, the clockwise angle from the P direction to the aircraft's forward axis is $(\varepsilon - \varepsilon^*) + (\psi_g - \psi_g^*) + \alpha$, where α is the clockwise angle from the roll axis of the platform to the roll axis of the aircraft.

The vectors P-P' and Q-Q' are components of the aircraft field corrections in this coordinate system. The measured magnetic heading ψ^* of the P-coordinate direction is given by

$$\psi^* = \psi_g^* - D_g^* \qquad 3$$

The true magnetic heading for purposes of analysing swing results (determining aircraft fields when values of D and H are given) is

$$\psi = \lambda_e + \varepsilon^* + \psi_g^* - D \qquad 4$$

The apparent magnetic heading is simply

$$\psi' = \psi^* - d_o \qquad 5$$

As mentioned above, these "headings" are within a few degrees of the respective aircraft headings.

CALIBRATION AND AIRCRAFT-FIELD CORRECTIONS, PERMANENT AND INDUCED

1. General Case

The effects of both aircraft-field corrections P-P' and Q-Q' and calibration corrections h_o and d_o can be combined (see Figure 3) to yield

$$P-P_o^* = aP + bQ + cZ + P_0 \qquad 6$$

$$Q-Q_o^* = dP + eQ + fZ + Q_0 \qquad 7$$

$$Z-Z^* = gP + hQ + kZ + R_0 \qquad 8$$

where

$$P = H \cos \psi \qquad 9$$

$$Q = -H \sin \psi \qquad 10$$

$$P_o^* = (H^* + h_o) \cos \psi^* \qquad 11$$

$$Q_o^* = -(H^* + h_o) \sin \psi^* \qquad 12$$

and a, b, ..., k are coefficients resulting from induced aircraft fields and from the angle d_o, and P_0, Q_0, and R_0 are constants resulting from permanent fields. Note that P_o^* and Q_o^* are components of the vector $H^* + h_o$, which equals H' in magnitude, not simply of the vector H*.

The actual coefficients in Equations 6 and 7 in terms of d_o and in terms of the induced coefficients a, b, ..., k, can be seen for example in Haines and Hannaford (1978), Equations 38 and 39 with $P'' = P_o^*$, $Q'' = Q_o^*$, $a_1 = b_2 = \cos d_o$, $a_2 = -b_1 = \sin d_o$, $a_3 = b_3 = 0$. However, since the effects cannot be separated, Equations 6 and 7 are the most general. In fact, they also include effects due to magnetometer orientation (ibid, page 7).

2. No Z variation over swings

If there is little variation in Z over the swing areas, the effect of the Z-induced fields must be combined with that of the respective permanent fields (see Haines and Hannaford, 1978). Denoting these combined effects as constants P_1, Q_1, and R_1:

$$P-P_o^* = aP + bQ + P_1 \qquad 13$$

$$Q-Q_o^* = dP + eQ + Q_1 \qquad 14$$

$$Z-Z^* = gP + hQ + R_1 \qquad 15$$

As before, the coefficients a, b, d, and e include not only the effects of induced aircraft fields and magnetometer orientation, but also of the angle d_o.

Expressing Equations 13 and 14 in terms of H*, ψ^*, H, and ψ (where ψ^* and ψ are given by Equations 3 and 4):

$$H \cos \psi - H^* \cos \psi^* = P_1 + h_o \cos \psi^* + aH \cos \psi - bH \sin \psi \qquad 16$$

$$-H \sin \psi + H^* \sin \psi^* = Q_1 - h_o \sin \psi^* + dH \cos \psi - eH \sin \psi \qquad 17$$

These equations are exact and are linear in the unknowns h_o, a, b, d, and e. Hence they can be solved directly by the normal method of least-squares. Of course, the two equations are coupled through the unknown h_o, and must be solved simultaneously.

Haines and Hannaford (1978, Equations 25 and 26) gave the same expressions with the exception that a term explicitly involving d_o was included, as well as induced terms a, b, d, and e. As a result, only 4 of the 5 unknowns could be determined. This is as

mentioned above - the effects of d_o and of induced fields are indistinguishable and so any 4 unknowns include the effect of the 5th. The equations (25 and 26) in Haines and Hannaford (1978), however, are only approximate (in order to make them linear in the parameter d_o), making it appear as though only d_o, b, and d are related, the (smaller) relation of a and e disappearing through the error terms.

The survey data can be corrected, given the least-squares values of h_o, a, b, P_1, d, e, Q_1, g, h, R_1 from Equations 13 to 15 (or equivalently, 15 to 17) by the inverse relationships

$$P = \frac{(1-e)(P_o + P_1) + b(Q_o + Q_1)}{(1-a)(1-e) - bd} \qquad 18$$

$$Q = \frac{(1-a)(Q_o + Q_1) + d(P_o + P_1)}{(1-a)(1-e) - bd} \qquad 19$$

$$Z = (Z^* + R_1) + gP + hQ \qquad 20$$

The corrected values ψ, H, and D are:

$$\psi = \arctan(-Q/P) \qquad 21$$

$$H = \sqrt{P^2 + Q^2} \qquad 22$$

$$D = \lambda_e + \varepsilon^* + D_g^* + \psi^* - \psi \qquad 23$$

where the arctangent must be taken in the quadrant appropriate to the signs of P and Q.

The F correction is given (see Haines and Hannaford, 1978, Equation 30) by

$$F-F^* = \left[a\cos^2\psi - (b+d)\sin\psi\cos\psi + e\sin^2\psi\right]H^2/F + \left[P_2\cos\psi - Q_2\sin\psi\right]H/F + R_1Z/F \qquad 24$$

$$= \left[\left(\frac{a+e}{2}\right) + \left(\frac{a-e}{2}\right)\cos 2\psi - \left(\frac{b+d}{2}\right)\sin 2\psi\right]H^2/F + \left[P_2\cos\psi - Q_2\sin\psi\right]H/F + R_1Z/F \qquad 25$$

where P_2 results from combining the effects of gZ and P_1, and Q_2 from combining hZ and Q_1.

The parameters derived in this section, based on swing observations taken where there is little variation in Z, must of course be used for correcting data over the entire survey. Over this survey, for example, the largest value of Z was about 3,500 nT above the swing value, the least was about 9,000 nT below. Since the error in approximating Equations 6 to 8 by Equations 13 to 15 is respectively c, f, and k times the amount Z varies from the swing Z, this error could be appreciable.

3. No H or Z variation over swings

It will be noticed that the solution of Equations 16 and 17 depends on the variation of H as well as of ψ. When swings are done at one location only, the h_o and aH terms are indistinguishable in Equation 16, because ψ and ψ^* are nearly equal. Similarily, the h_o and eH terms are indistinguishable in Equation 17. The equations, under these conditions, become

$$H\cos\psi - H^*\cos\psi^* = P_1 + (h_o + aH)\cos\psi - bH\sin\psi + \varepsilon_1 \qquad 26$$

$$-H\sin\psi + H^*\sin\psi^* = Q_1 - (h_o + eH)\sin\psi + dH\cos\psi + \varepsilon_2 \qquad 27$$

where

$$\varepsilon_1 = h_o(\cos\psi^* - \cos\psi) \qquad 28$$

$$\varepsilon_2 = -h_o(\sin\psi^* - \sin\psi) \qquad 29$$

It can be shown that the maximum value of $|\varepsilon_1|$ and $|\varepsilon_2|$ is $2h_o\sin\left|\frac{D-D^*}{2}\right|$. In this survey the maximum error was about 3 nT, and so ε_1 and ε_2 could be neglected.

Thus in this case, when there is little H or Z variation over the swings, the least-squares equations become uncoupled, with 3 unknowns in each. Of course, as in the case of no Z variation, correcting survey data on the basis of a collapsed model such as this would be undesirable if there were large H variations over the survey, since large errors could result when H at the survey location differed greatly from H at the swing location. Over this survey, for example, the largest value of H was about 5,000 nT above the swing value, the least was about 8,500 nT below. Thus the errors in approximating Equations 16 and 17 by Equations 26 and 27 could be quite large, depending respectively on the sizes of a and e. Furthermore, the errors resulting from no H variation over the swing areas are in addition to the errors discussed in the last section, resulting from no Z variation over the swing areas.

The Z-correction (Equation 15) remains the same when there is no H-variation over the swings. In the case of the F-correction (Equation 25) the $\left(\frac{a+e}{2}\right)H^2/F$ and R_1Z/F terms are indistinguishable and must be combined. Again, this could cause errors when correcting F over the survey.

CALIBRATION AND AIRCRAFT-FIELD CORRECTIONS, PERMANENT ONLY

When the coefficients a, b, d, e arise only from the angle d_o, it can be shown that

$$a = 1 - \cos d_o \quad (30)$$

$$b = -\sin d_o \quad (31)$$

$$d = \sin d_o \quad (32)$$

$$e = 1 - \cos d_o \quad (33)$$

Substituting these equations into Equations 16 and 17 yields

$$\cos d_o \, H \cos \psi - (H^* + h_o) \cos \psi^* = P_1 + \sin d_o \, H \sin \psi \quad (34)$$

$$-\cos d_o \, H \sin \psi + (H^* + h_o) \sin \psi^* = Q_1 + \sin d_o \, H \cos \psi \quad (35)$$

These equations, although exact, are non-linear in the parameter d_o. They are coupled through both h_o and d_o, and can be solved readily by non-linear least-squares methods.

The solution of these equations can be tested statistically against, and as a result possibly replace, the solution of Equations 16 and 17 (no Z variation) or Equations 26 and 27 (no H or Z variation).

The survey data are corrected, when there are no induced fields, by determining:

$$P = \cos d_o \, (P_o^* + P_1) - \sin d_o \, (Q_o^* + Q_1) \quad (36)$$

$$Q = \sin d_o \, (P_o^* + P_1) + \cos d_o \, (Q_o^* + Q_1) \quad (37)$$

$$Z = Z^* + R_1 \quad (38)$$

$$F = F^* + R_1 \, Z/F + (P_2 \cos \psi - Q_2 \sin \psi) \, H/F \quad (39)$$

and using Equations 21 to 23 as before.

SWING-DERIVED CORRECTIONS

The method of swing-derived corrections has been explained in detail by Haines and Hannaford (1976).

During this survey three swing flights were made over Rosaire, Quebec: one swing flight consisting of 10 passes at the beginning of the survey (Flight 1), one consisting of 10 passes in the middle (Flight 11), and one consisting of 12 passes at the end (Flight 26). There was also one pass during Flight 5, but in this case only the proton F measurement could be used since the platform was not horizontal and so the fluxgate D, H, and Z measurements were invalid.

Since all swing observations were taken at one location, the equations to be used for both permanent and induced aircraft fields are those of the subsection dealing with no H or Z variations over swings. The equations for permanent fields only are those of the last section. The solution from the latter can be tested statistically against the former, to determine whether they are sufficient in explaining the variation in the observations. Both sets of equations of course include the effects of the calibration corrections h_o and d_o.

The induced fields were in fact found to be statistically insignificant. Also, the forward components of the aircraft field, both P_1 at the fluxgate and P_2 at the proton sensor, were statistically insignificant. The calibration corrections for the fluxgate system and the remaining permanent-field corrections for the two magnetometer systems, with the standard errors affixed as $\pm$ quantities, were found to be as follows:

Fluxgate Magnetometer

$d_o = -1.42 \pm .09°$
$h_o = 61 \pm 25$ nT
$Q_1 = -322 \pm 25$ nT
$R_1 = 50$ nT

Proton Magnetometer

$Q_2 = -28 \pm 7$ nT
$R_1 = -12.1 \pm 1.6$ nT

The swing values H-H' and H(D-D') are plotted against magnetic heading ψ in the top diagram of Figure 4. The least-squares correction curve, for H = 15 950 nT (the mean value at Rosaire), is also shown. The scatter of the 64 points about their least-squares curve is 142 nT.

The bottom diagram of Figure 4 shows Z-Z' corrected for the following "swing-constant" R_1:

Flight	R_1	St. error
1	-14 nT	16 nT
11	18	16
26	83	14

That is, Z-Z' varies with time, and to investigate any heading effect (coefficients g and h in Equation 15) this time-effect must first be removed. The heading effect was not statistically significant. The scatter of the 32 points, after removal of these individual flight means, is 49 nT.

The given "swing-derived" value of 50 nT for R_1 comes not from taking a simple or weighted mean, but from estimating the mean over the entire survey. A "consistency-derived" Z-correction, which will be discussed later, is applied after the swing-derived corrections are applied, and cancels any error in the swing-derived R_1.

The F-F' values for the proton magnetometer, and the resulting least-squares correction curve, are shown in Figure 5. The scatter of the 33 points about their least-squares curve is 8.6 nT.

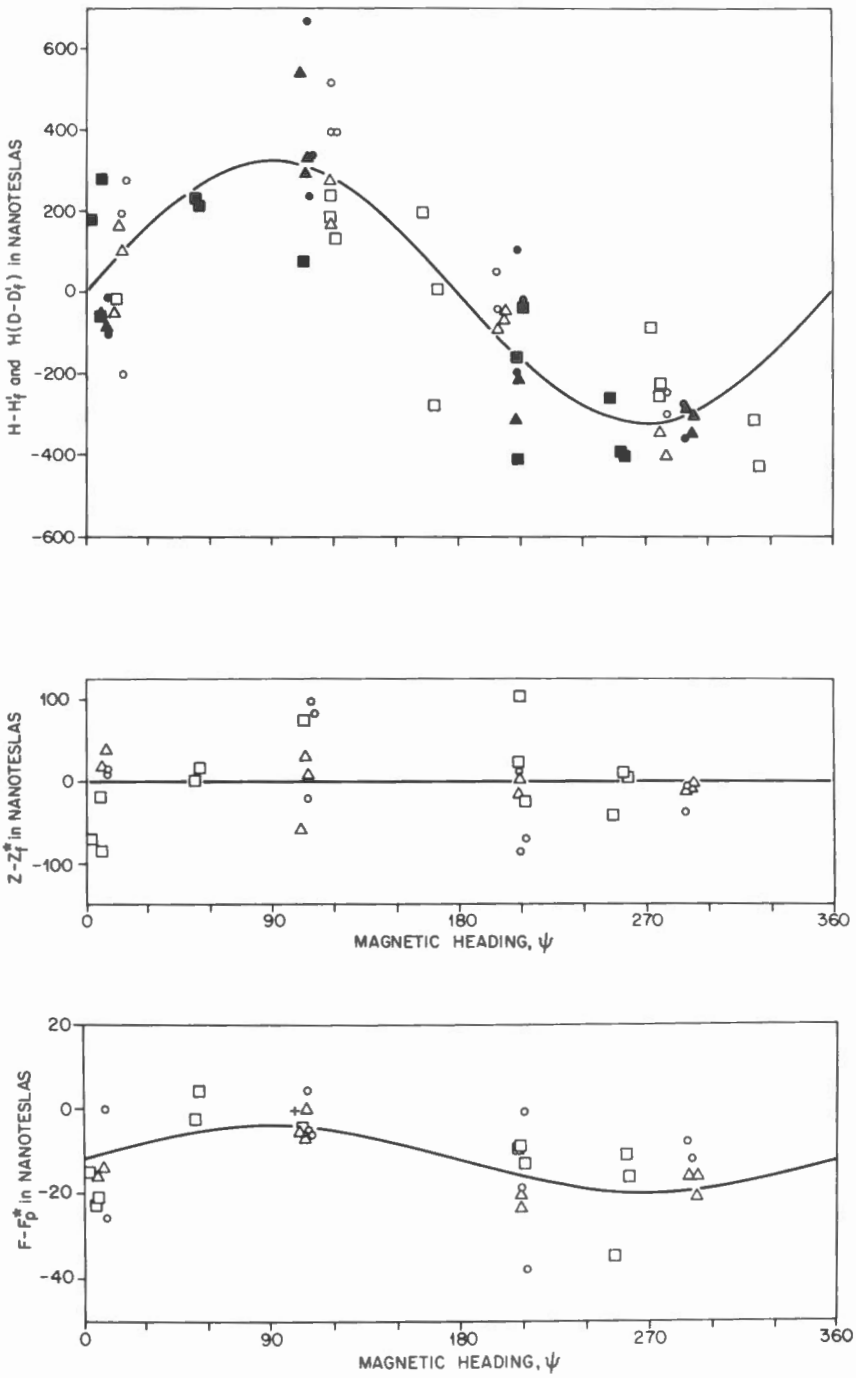

Fig. 4

Swing-derived corrections to fluxgate-measured H and D, and to fluxgate-measured Z after removal of "swing-constant" values for R_1. Circles, triangles, and squares apply to Rosaire swing flights 1, 11, and 26, respectively. In top diagram the solid symbols are H-H' plotted at magnetic heading ψ, the open symbols are H(D-D') plotted at $\psi - 90°$. The H correction curve at Rosaire (H = 15 950 nT) is shown.

Fig. 5

Swing-derived corrections to proton-measured F. Circles, triangles, and squares apply to Rosaire swing flights 1, 11, and 26; plus sign applies to single Rosaire pass during flight 5. Correction curve at Rosaire (H = 15 950 nT) is shown.

CONSISTENCY-DERIVED CORRECTIONS FOR Z

The method of determining and applying a time-varying "consistency-derived" Z correction δR has been explained by Haines and Hannaford (1978). The overall Z correction is

$$Z - Z^* = gH \cos\psi - hH \sin\psi + R_1 + \delta R \qquad 40$$

where g and h are induced coefficients (found for this survey to be statistically insignificant and taken to be zero), and R_1 is the swing-derived Z-correction (chosen for this survey to be 50 nT).

Figure 6 shows the time-varying difference between the total field F_p as measured by the proton magnetometer and the total field $F_f = \sqrt{H^2 + Z^2}$ as measured by the fluxgate magnetometer. This time-varying difference is taken as the consistency-derived Z correction δR.

Taking $(F_p - F_f)$ as the Z-correction δR is of course an approximation, the actual expression for δR being (ibid, Equation 59):

$$\delta R = F/Z\,(F_p - F_f) - \delta P\,(H/F)\cos\psi + \delta Q\,(H/F)\sin\psi \qquad 41$$

where δP and δQ are the unknown variations in the horizontal P and Q fields. The terms involving δP and δQ are generally small, because of the H/Z factor. Their magnitudes can be estimated by taking half the differences between the $F_p - F_f$ before and after turns of approximately 180°. They are found to be small: the mean magnitude of $\delta P\,(H/F)\cos\psi - \delta Q\,(H/F)\sin\psi$ from 24 turns was 8 nT, and the scatter was 7 nT. Also, the F/Z factor was taken as unity which results in an error of only 1 or 2 nT. This latter error is quite acceptable and indeed is much smaller than the average error resulting from putting $\delta P = \delta Q = 0$.

The mean of over 15000 $F_p - F_f$ values from this survey, after the consistency-derived corrections were applied, was 0.9 nT and the scatter was 6.2 nT.

Note that the consistency-derived δR corrects for any error in the swing-derived R_1.

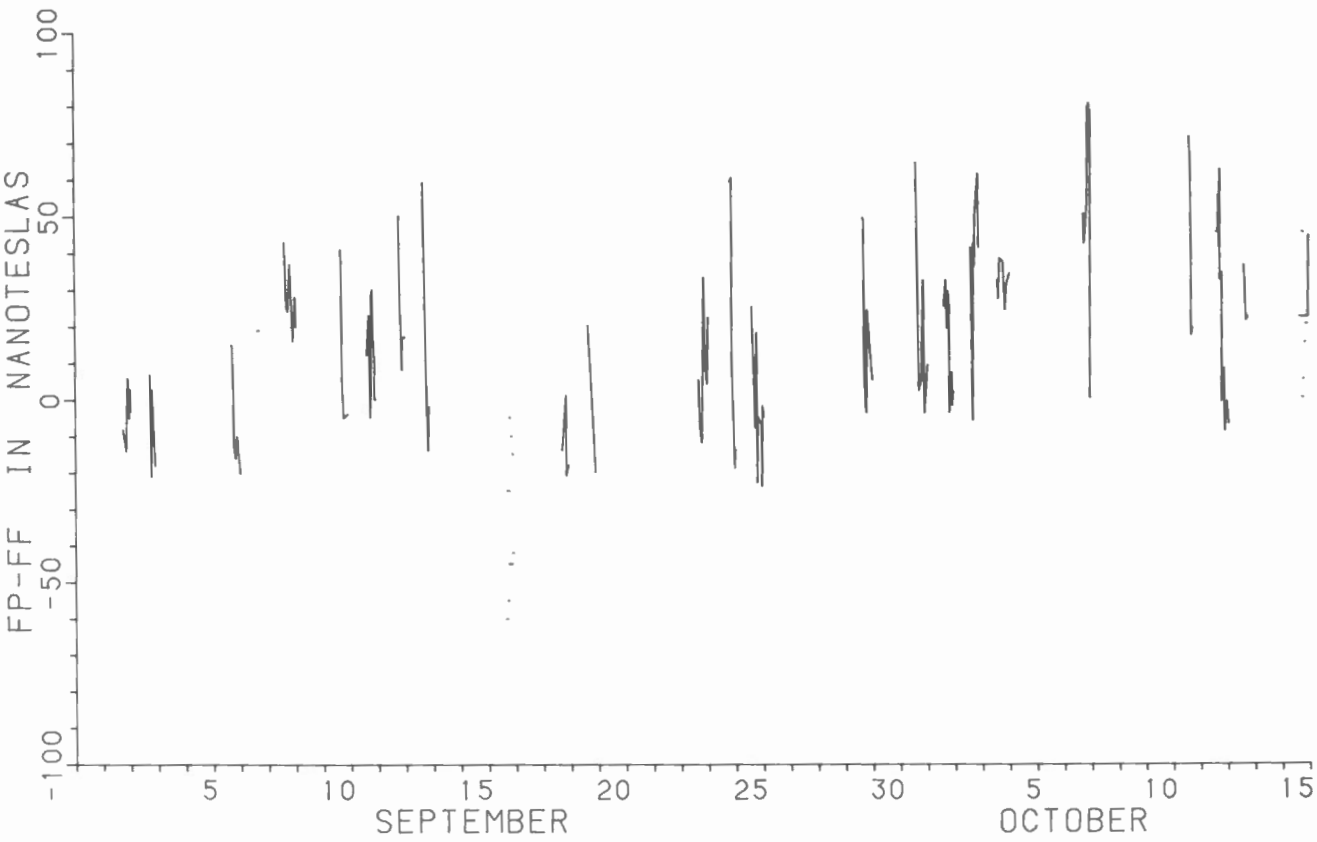

Fig. 6 Plot of $F_p - F_f$ for 1976 aeromagnetic survey. This time-varying function was taken as the consistency-derived Z-correction (δR).

CONSISTENCY OF DATA FROM THE TWO MAGNETOMETER SYSTEMS

The two magnetometers gave separate measurements of the total field, the proton magnetometer measuring F_p directly and the fluxgate magnetometer measuring F_f through H_f and Z_f.

Since the F_p measurement was of much higher accuracy than the F_f measurement, F_p was chosen whenever it was available. Also, because of the higher F_p accuracy and because Z is fairly close to F over the survey area, the calculation $F_p^2 - H_f^2$ has a higher accuracy than Z_f. This in fact is the basis of the consistency-derived Z-correction δR. Thus, whenever F_p and H_f are both available, the vertical field (Z_{pf}, say) is calculated from them. This automatically ensures data consistency in the sense that $H_f^2 + Z_{pf}^2 = F_p^2$.

However, when F_p is not available, and F_f is, it is necessary to ensure that F_f agrees with F_p in the sense that there be no level shift when the F changes from F_p to F_f. Similarly when H_f and F_p are not both available, but Z_f is, there should be no level shift as Z changes from Z_{pf} to Z_f.

The elimination of any significant level differences in Z and F, as data from the two magnetometers are combined, is accomplished by the consistency - derived Z-correction δR. Thus, although Z_f is discarded in favor of Z_{pf} when H_f, Z_f, and F_p are all available, it is nevertheless used in determining the $F_p - F_f$ values from which is derived the δR correction as a function of time. This δR can then be used as a correction to Z_f when F_p and H_f are not both available. The 1 nT mean and 6 nT scatter of the $F_p - F_f$ values is believed to be an indication of the final level differences between F_f and F_p, and between Z_f and Z_{pf}.

For the survey, only 5% of the final F values and 14% of the final Z values came from the fluxgate magnetometer. The number of 30-second averages in the various measurement combinations are as follows (the derived element is in brackets):

Combination	Number of averages
Z_f	106
H_f Z_f (F_f)	16
D_f H_f Z_f (F_f)	794
F_p	1,672
D_f H_f F_p (Z_{pf})	105
Z_f F_p	1,371
H_f Z_f F_p (Z_{pf})	54
D_f H_f Z_f F_p (Z_{pf})	13,340
Total	17,458

The Z_f in the last two combinations are replaced by the derived Z_{pf}. Note also that a horizontal intensity is not derived from the Z_f and F_p combination, since the resulting error would be unacceptable.

PRESENTATION OF DATA

Haines and Hannaford (1976) described the recording of 3-second raw data, the process of editing and massaging them, and the forming and statistical editing, by computer, of the 30-second averages. Haines and Hannaford (1978) described the technique and criteria used in determining whether the field is sufficiently disturbed to require data rejection. The accepted 30-second averages are finally corrected for calibration errors and aircraft fields, as described earlier.

A polynomial in two spatial coordinates was fitted to each of three orthogonal components U, V, and Z, after reducing the data to sea level by means of the "inverse-cube relationship" (see for example Haines and Hannaford, 1976). The horizontal components U and V are defined by:

$$U = H \cos \left[D - (\lambda - \lambda_o)\right] \qquad 42$$

$$V = H \sin \left[D - (\lambda - \lambda_o)\right] \qquad 43$$

where λ is the geographic east longitude and λ_o is a map rotation angle, chosen for this survey to be -180°.

The standard errors of estimate of least-squares fits to 1st, 2nd, 3rd, and 4th degree polynomials, and to the adopted 3rd degree polynomials with significant terms only, are given in Table I.

Coefficients for the adopted 3rd degree polynomials are given in Table II. Definitions of the spatial coordinates and of the components U, V, and Z, as well as formulae relating U and V to the more familiar D, H, X, and Y, are also given in the Table.

A comparison of the International Geomagnetic Reference Field (IGRF) with the 3rd degree polynomial field of Table II is given in Figure 7. There are large biases in the IGRF over the area, as there are over areas of previous surveys (Haines and Hannaford, 1972, 1974, 1976, and 1978.)

Profile plots of 1/2-minute IGRF residuals in D, H, Z, X, Y, and F are shown in Figures 8 to 13. A residual is a 1/2-minute average (corrected for calibration errors and permanent aircraft fields) minus the corresponding IGRF value for 1976.7 at the altitude of observation. The residuals, represented by the short lines joining the profile to the flight track, are plotted normal to the track, positive residuals being plotted in the upper right half-plane, negative in the lower left (see circular scale in title block: radially gridded area defines area of positive residuals). Because of the scale reduction required for page-size publication, only every second residual was joined to the track.

The plots were produced entirely by computer, on a scale of 1:5,000,000. The coastline data-set is not accurate (in some places it is out by 35 km) and so anomalies should be located by using the latitude-longitude grid rather than the coastline.

TABLE I

Standard deviations in nanoteslas of observed minus polynomial fields of 1st, 2nd, 3rd, and 4th degree, and the adopted 3rd-degree with significant terms only (denoted by 3 sig). Coefficients column gives total number of coefficients in the three polynomials. Sample size = 1424 for U and V, 1577 for Z (every tenth 30 second average)

Degree	Coefficients	U	V	Z
1	9	235.7	277.4	604.5
2	18	141.9	175.9	166.0
3	30	140.7	164.1	158.1
4	45	139.9	163.7	155.9
3 sig	26	140.7	164.3	158.1

TABLE II

3rd degree polynomial reference field in nanoteslas for 1976.7 at sea level.

$U = \Sigma u_i x_i \qquad V = \Sigma v_i x_i \qquad Z = \Sigma z_i x_i$

$a = -K \tan(\theta/2) \cos(\lambda - \lambda_o) - a_o$
$b = K \tan(\theta/2) \sin(\lambda - \lambda_o) - b_o$

θ = colatitude
λ = east longitude
K = 100.
λ_o = -180°
a_o = 17.2
b_o = 27.6

$D = \arctan(V/U) + (\lambda - \lambda_o)$
$H = (U^2 + V^2)^{1/2}$
$X = U \cos(\lambda - \lambda_o) - V \sin(\lambda - \lambda_o)$
$Y = U \sin(\lambda - \lambda_o) + V \cos(\lambda - \lambda_o)$

i	x_i	u_i	v_i	z_i
1	1	-12574.51	-6424.86	54688.41
2	a	-579.841	5.846	-570.272
3	b	-48.080	-547.847	-3.265
4	a^2	5.8275	-1.7265	-9.6514
5	ab	-5.3429	8.6736	-5.6998
6	b^2	4.1649	-6.9881	-12.8409
7	a^3			.09716
8	a^2b	.08556		-.21247
9	ab^2	.08318		.39113
10	b^3	.05327	.32415	-.18687

Note: Coefficients that were statistically insignificant are left blank, and are taken as zero.

ACKNOWLEDGMENTS

The authors wish to thank Conair Aviation Ltd. for their cooperation in conducting the survey and in particular to acknowledge the help of Captains D. Maclagan and A. Melhof and Navigator A. Lyon.

The airborne scientific crew comprised Earth Physics Branch personnel F. Andersen, G. Carr, R. Charbonneau, and W. Hannaford. A ground station at Rosaire, Québec, was operated at the beginning of the survey by G. Massie and L. Newitt and at the end of the survey by E. Berndt and M. Gervais.

G. Jansen van Beek and E. Loomer provided Ottawa Observatory values for ground value control for the Rosaire swings, and magnetograms used in checking for magnetic disturbances during the survey.

R.L. Coles assisted in the determination of the magnetically disturbed time intervals for purposes of data rejection.

The authors wish to thank Dr. R.L. Coles and Dr. P.H. Serson for reviewing the manuscript.

REFERENCES

Haines, G.V. and W. Hannaford, 1972. Magnetic anomaly maps of British Columbia and the adjacent Pacific Ocean. Pub. Earth Phys. Br., Vol. 42, No. 7, pp. 211-228.

Haines, G.V. and W. Hannaford, 1974. A three-component aeromagnetic survey of the Canadian Arctic. Pub. Earth Phys. Br., Vol. 44, No. 8, pp. 209-234.

Haines, G.V. and W. Hannaford, 1976. A three-component aeromagnetic survey of Saskatchewan, Alberta, Yukon and the District of Mackenzie. Geomagnetic Service of Canada, Geomag. Series No. 8, 34 p.

Haines, G.V. and W. Hannaford, 1978. A three-component aeromagnetic survey of central Canada. Geomagnetic Service of Canada, Geomag. Series No. 13, 28 p.

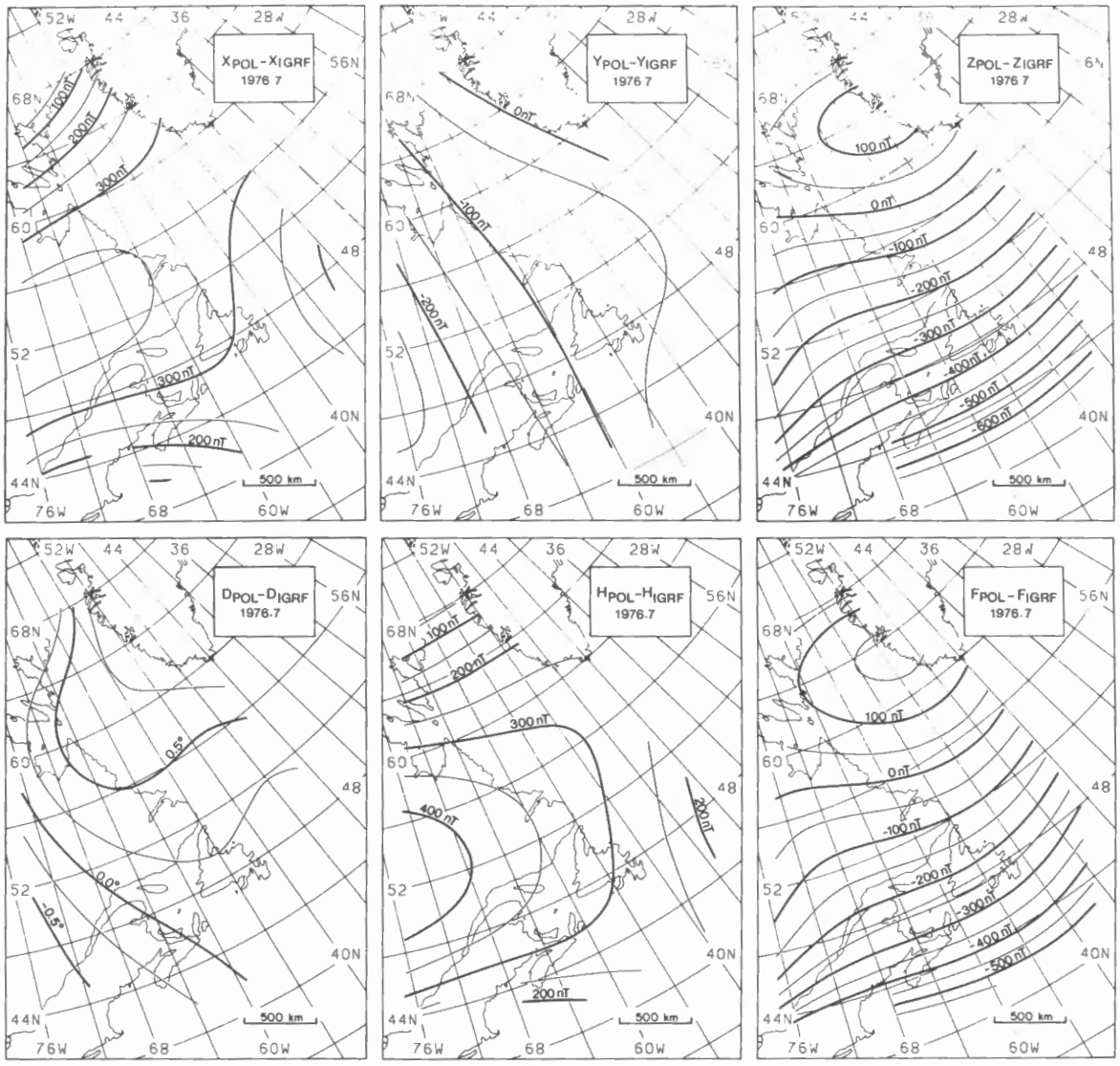

Fig. 7 Comparison of International Geomagnetic Reference Field (IGRF) with adopted 3rd degree polynomial (POL).

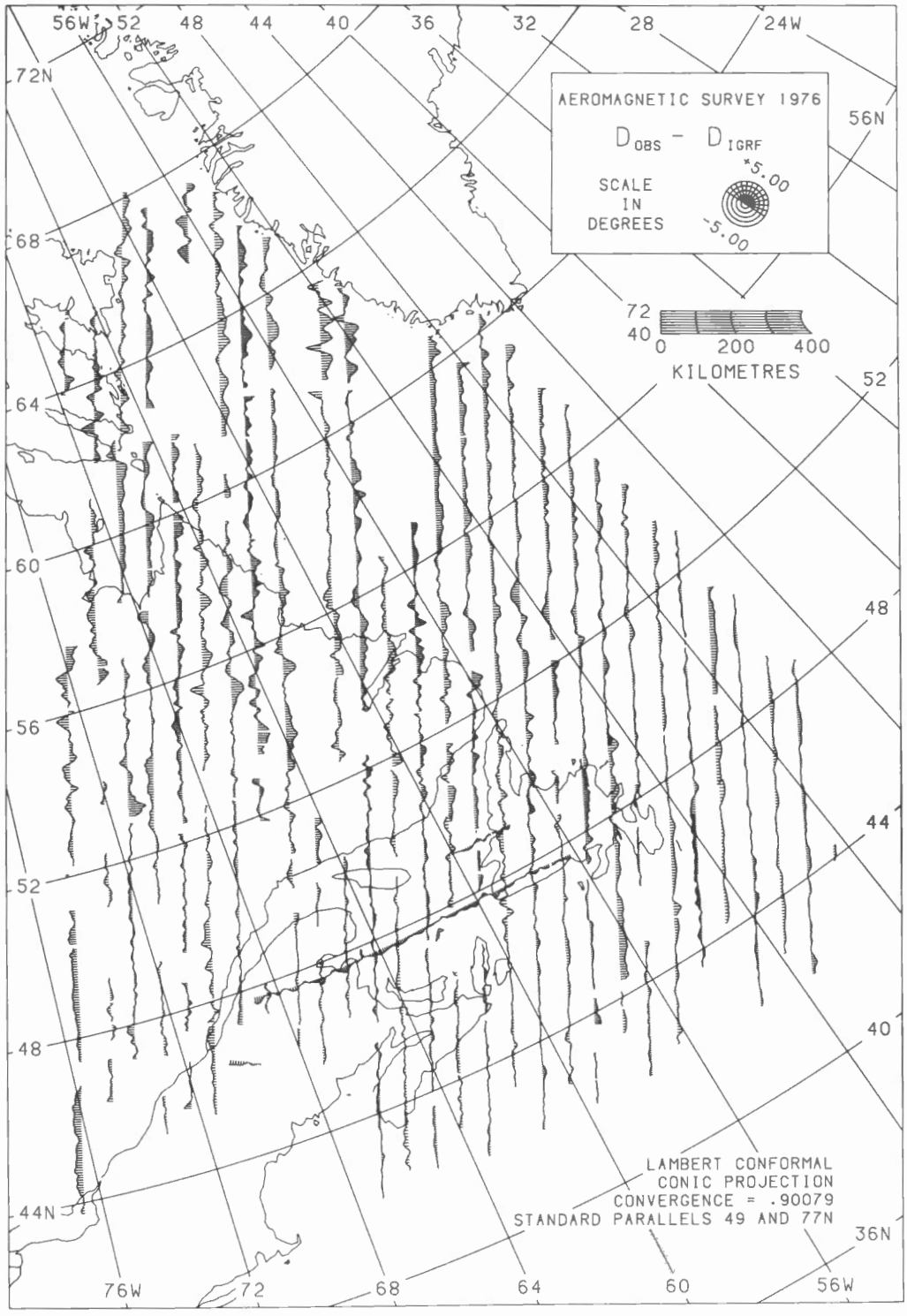

Fig. 8

Residual profiles of declination D, relative to the International Geomagnetic Reference Field (IGRF) at 1976.7. The residuals are 1/2 minute averages (corrected for calibration errors and aircraft fields) minus the corresponding IGRF values for 1976.7 at the altitude of observation. Residuals are plotted normal to the flight track, positive residuals in the upper right half-plane (radially gridded part of circular scale) and negative residuals in the lower left. Only every second residual is joined to the flight track. The residual profile plots were produced entirely by computer, and the coastline is inaccurate in some places. Hence anomalies should be located by referring to the latitude-longitude grid.

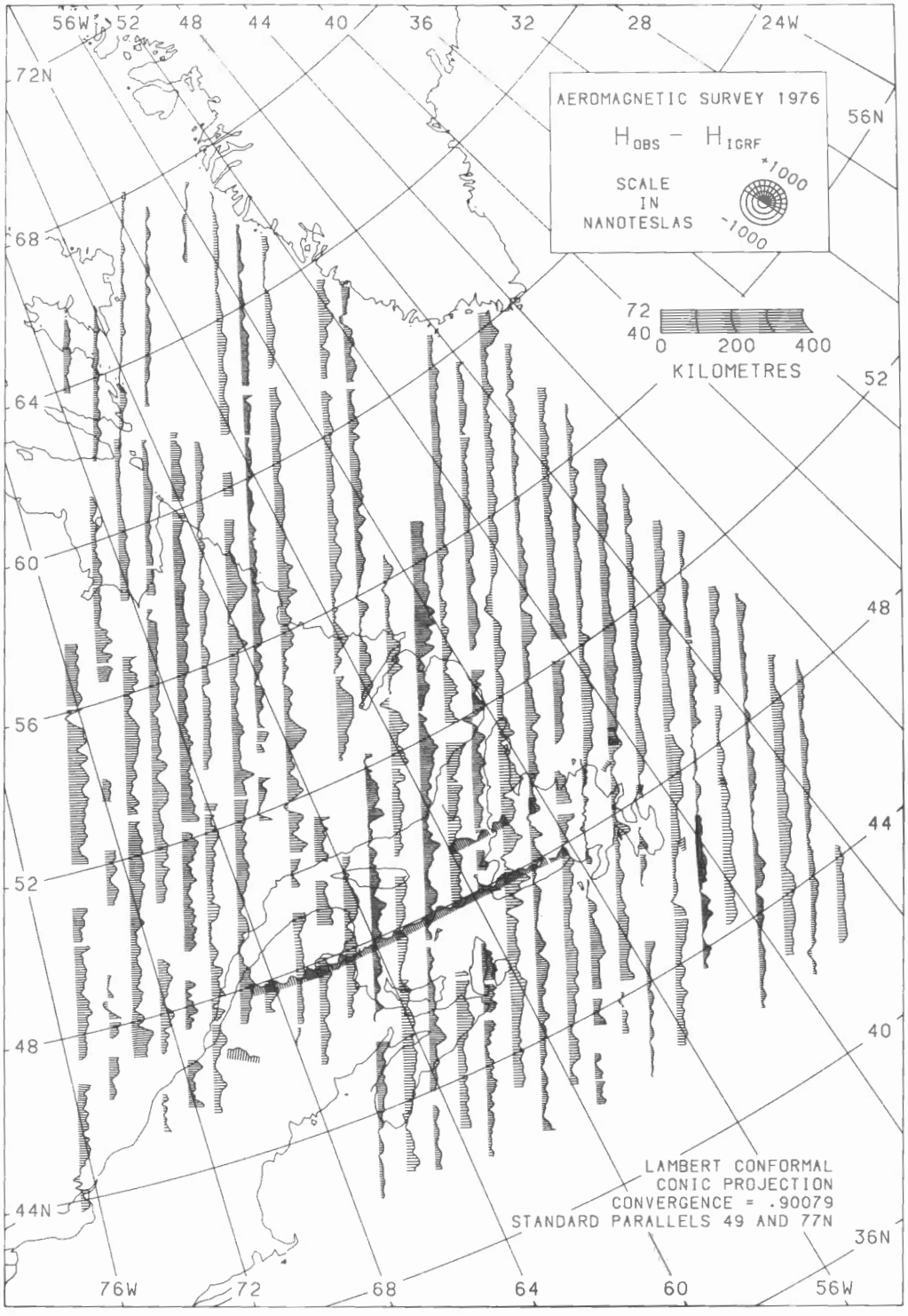

Fig. 9 Residual profiles of horizontal intensity H, relative to the IGRF at 1976.7.

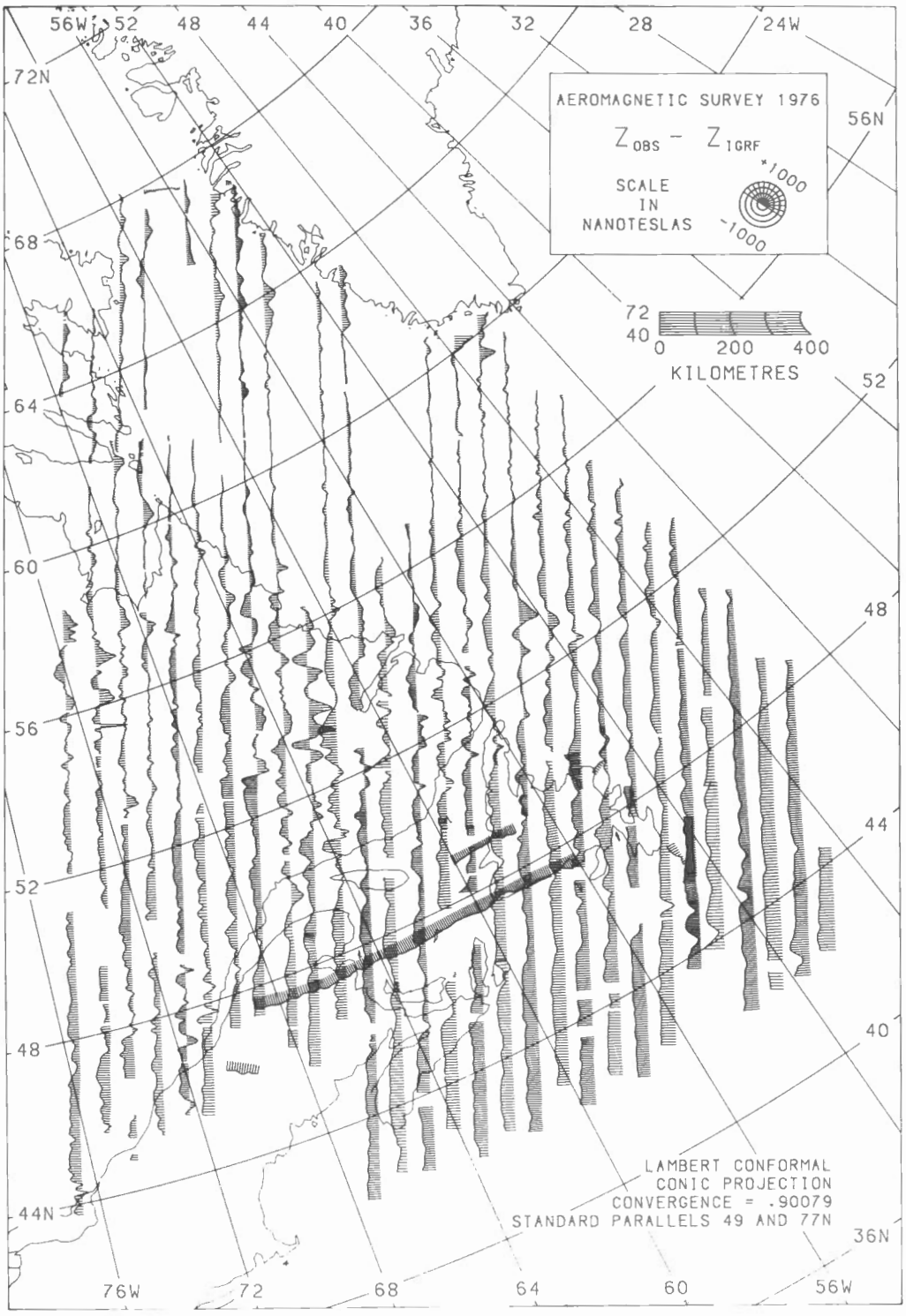

Fig. 10 Residual profiles of vertical intensity Z, relative to the IGRF at 1976.7.

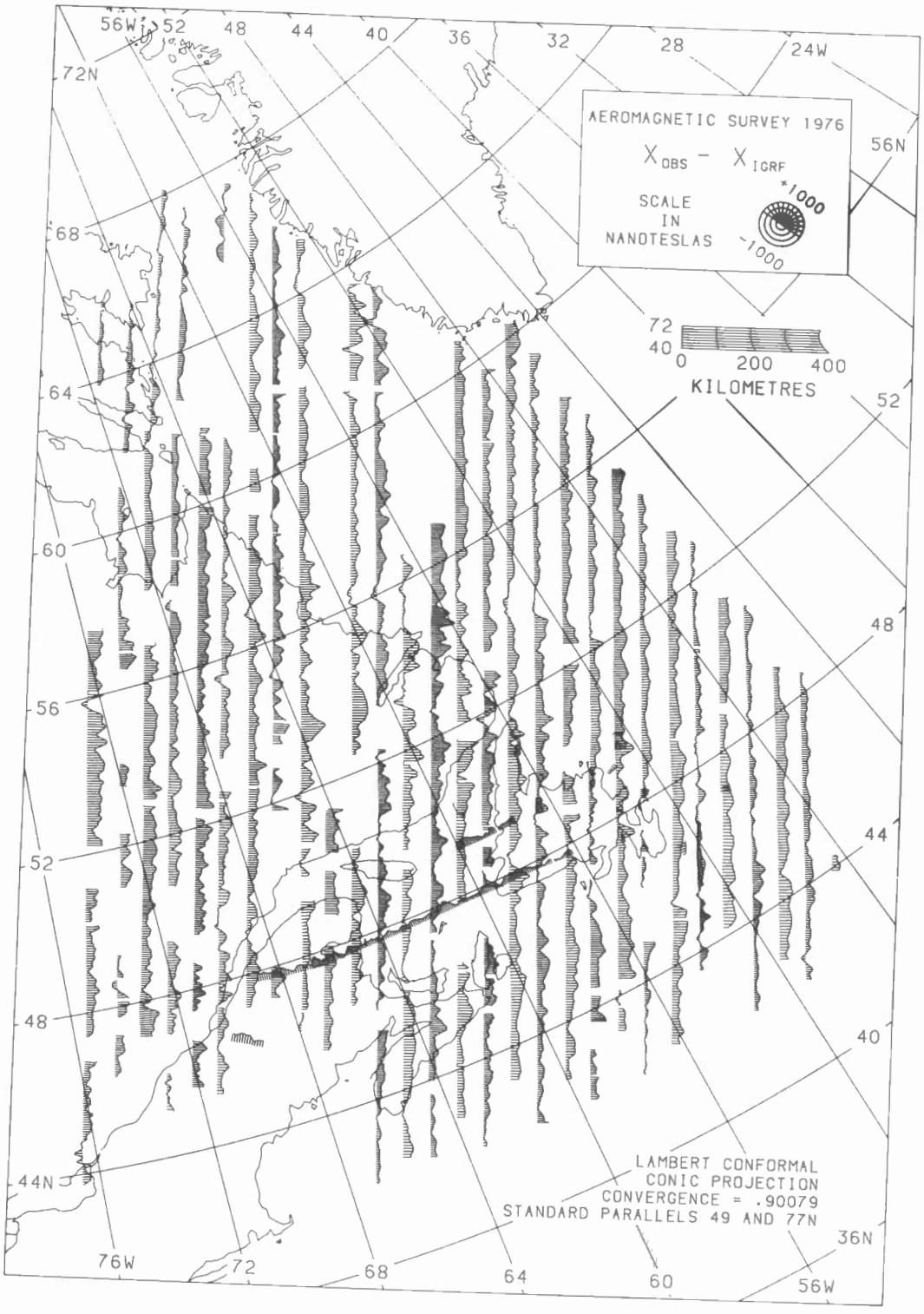

Fig. 11 Residual profiles of geographic north component X, relative to the IGRF at 1976.7.

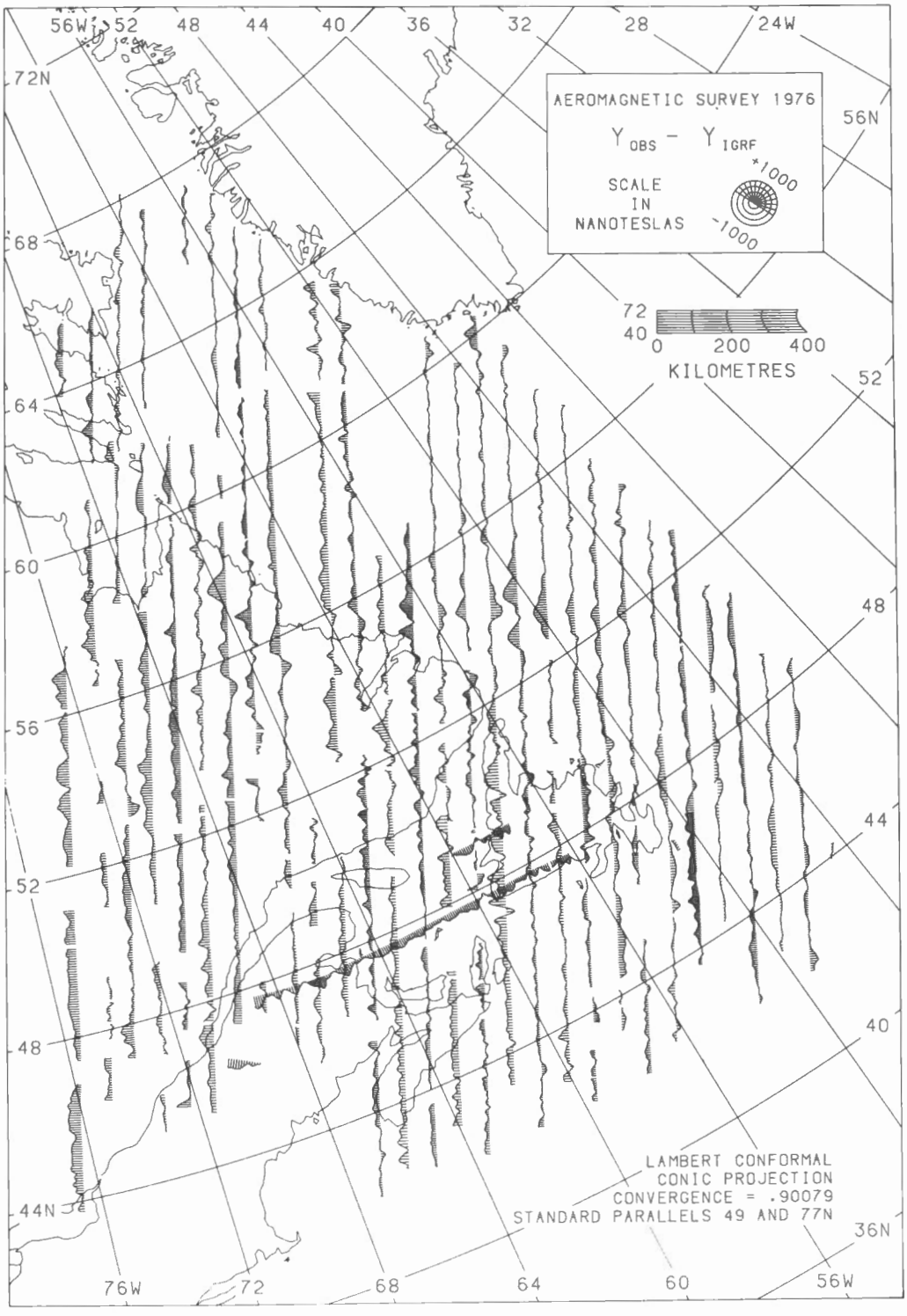

Fig. 12 Residual profiles of geographic east component Y, relative to the IGRF at 1976.7.

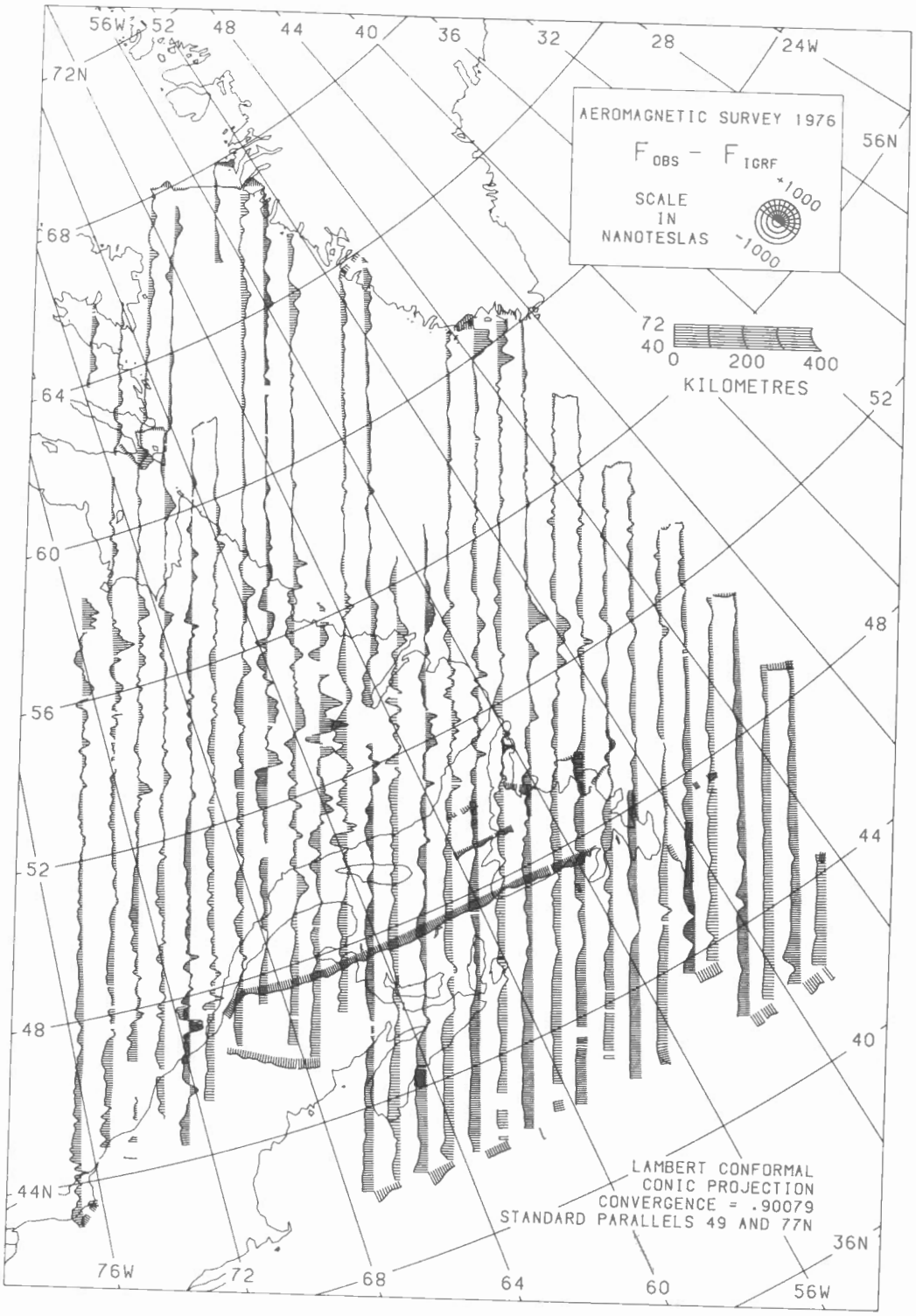

Fig. 13 Residual profiles of total intensity F, relative to the IGRF at 1976.7.